

Lithium abundance in the globular cluster M4: from the Turn-Off to the RGB Bump ^{*}

A. Mucciarelli,¹ M. Salaris,² L. Lovisi,¹ F.R. Ferraro,¹ B. Lanzoni,¹
S. Lucatello,^{3,4} and R.G. Gratton³

¹*Dipartimento di Astronomia, Università degli Studi di Bologna, Via Ranzani, 1 - 40127 Bologna, ITALY*

²*Astrophysics Research Institute, Liverpool John Moores University, 12 Quays House, Birkenhead, CH41 1LD, United Kingdom*

³*INAF- Osservatorio Astronomico di Padova, Vicolo dell'Osservatorio 5, I-35122 Padova, Italy*

⁴*Excellence Cluster Universe, Technische Universität München, Boltzmannstr. 2, 85748, Garching, Germany*

1 October 2018

ABSTRACT

We present Li and Fe abundances for 87 stars in the globular cluster M4, obtained by using high-resolution spectra collected with GIRAFFE@VLT. The targets range from the Turn-Off up to the Red Giant Branch Bump. The Li abundance in the Turn-Off stars is uniform, with an average value equal to $A(\text{Li}) = 2.30 \pm 0.02$ dex ($\sigma = 0.10$ dex), consistent with the upper envelope of Li content measured in other globular clusters and in the Halo field stars, confirming also for M4 the discrepancy with the primordial Li abundance predicted by WMAP+BBNS. The global behaviour of $A(\text{Li})$ as a function of the effective temperature allows to identify the 2 main drops in the Li evolution due to the *First Dredge-Up* and to the extra-mixing episode after the *Red Giant Branch Bump*. The measured iron content of M4 results to be $[\text{Fe}/\text{H}] = -1.10 \pm 0.01$ dex ($\sigma = 0.07$ dex), with no systematic offsets between dwarf and giant stars.

The behaviour of the Li and Fe abundance along the entire evolutionary path is incompatible with theoretical models including pure atomic diffusion, pointing out that an additional turbulent mixing below the convective region needs to be taken into account, able to inhibit the atomic diffusion. The measured value of $A(\text{Li})$ and its homogeneity in the Turn-Off stars allow to put strong constraints on the shape of the Li profile inside the M4 Turn-Off stars. The global behaviour of $A(\text{Li})$ with the effective temperature can be reproduced with different pristine Li abundances, depending on the kind of adopted turbulent mixing. One cannot reproduce the global trend starting from the WMAP+BBNS $A(\text{Li})$ and adopting the turbulent mixing described by Richard et al. (2005) with the same efficiency used by Korn et al. (2006a) to explain the Li content in NGC 6397. In fact such a solution is not able to well reproduce simultaneously the Li abundance observed in Turn-Off and Red Giant Branch stars. Otherwise, the WMAP+BBNS $A(\text{Li})$ can be reproduced assuming a more efficient turbulent mixing able to reach deeper stellar regions where the Li is burned.

We conclude that the cosmological Li discrepancy cannot be easily solved with the present, poor understanding of the turbulence in the stellar interiors and a future effort to well understand the true nature of this non-canonical process is needed.

Key words: stars: abundances – Stars: atmospheres – Stars: Population II – (Galaxy:) globular clusters: individual (M4)

1 INTRODUCTION

The determination of the initial Li abundance in low-mass, metal-poor, Population II stars is one of the most debated astrophysical topics. Li is one of the few elements synthesized during the primordial Big Bang nucleosynthesis (BBNS), and its initial abundance in metal poor stars sets constraints to the BBNS.

* Based on observations collected at the ESO-VLT under program 081.D-0356. Also based on observations collected at the ESO-MPI Telescope under program 69.D-0582, and with the NASA/ESA HST, obtained at the Space Telescope Science Institute, which is operated by AURA, Inc., under NASA contract NAS5-26555.

Li is a very fragile element, that is destroyed when the temperature is larger than $\sim 2.5 \cdot 10^6$ K through the ${}^7\text{Li}(p,\alpha){}^4\text{He}$ reaction. Hence, whenever Li is produced in the stellar interiors during hydrostatic burnings, it is immediately disintegrated. The discovery of a constant Li abundance in unevolved, Population II stars, the so-called *Spite Plateau* (Spite & Spite 1982) – has been interpreted as the signature of the primordial abundance of Li, produced during the BBNS. When the lithium abundance is expressed as $A(\text{Li}) = \log(n(\text{Li})/n(\text{H})) + 12$, the *Spite Plateau* turns out to be between 2.1 and 2.4, depending on the adopted T_{eff} scale (Bonifacio & Molaro 1997; Charbonnel & Primas 2005; Asplund et al. 2006; Bonifacio et al. 2007; Aoki et al. 2009).

The recent estimate of the cosmological baryon density obtained with the *Wilkinson Microwave Anisotropy Probe* (WMAP) satellite (Spergel et al. 2007) from the power spectrum of the cosmic microwave background fluctuations, throws into a crisis the classical interpretation of the *Spite Plateau*. In fact, by combining the WMAP results with standard BBNS calculations, the most recent estimate of Li is a primordial abundance $A(\text{Li}) = 2.72 \pm 0.06$ dex (Cyburt et al. 2008)¹. This value is significantly higher, by at least a factor of 3, than the Li abundance derived from metal-poor dwarfs.

At present, the WMAP+BBNS/*Spite Plateau* discrepancy is still unsolved and different possible solutions have been advanced and investigated: (1) an inadequacy of the standard BBNS treatment; (2) Population III stars could have been capable to destroy some of the pristine Li and Population II stars were born from a Li-depleted gas (Piau et al. 2006); (3) Li may be depleted in the photospheres of Population II stars (born with WMAP+BBNS Li abundance) by atomic diffusion: this process alters the surface chemical composition of the star, hiding a fraction of Li (but also He, Fe and other heavy elements) below the observable photospheric layers.

Galactic globular clusters (GCs) provide an alternative way to investigate the primordial Li abundance, for they host samples of stars approximately coeval, with uniform initial abundances of several elements – Fe among them – and whose evolutionary status is easily determined from photometry. Also, GCs offer the possibility to trace the diffusion effects along the entire evolutionary path of Population II stars. In fact, the amount of diffusion can be easily measured from the offset of the surface abundance of elements like Fe – that are not involved in nuclear burnings – between the turn off (TO) stars (where the diffusion affects appreciably the photospheric abundances) and the red giants (where convection restores the original photospheric abundances). Systematic differences between the Fe content of Sub Giant Branch (SGB) and red giant branch (RGB) stars have been detected in M92 (King et al. 1998) and in NGC 6397 (Lind et al. 2009b). On the other hand independent studies have found a high level of homogeneity in Fe and other elements in the latter cluster (Gratton et al. 2001) and in others (see also Castilho et al. 2000; Cohen & Meléndez 2005).

Extensive chemical screenings of Li content in GCs

dwarf stars have been until now limited to the few closest objects, namely 47 Tuc (Bonifacio et al. 2007; D’Orazi et al. 2010), NGC 6397 (Bonifacio et al. 2002; Korn et al. 2006a; González Hernández et al. 2009; Lind et al. 2009b), NGC 6752 (Pasquini et al. 2005) and M92 (Boesgaard et al. 1998; Bonifacio 2002). The metal-poor GC NGC 6397, in particular, has been recently the object of an intense debate regarding the discrepancy between cosmological and stellar Li abundance. Korn et al. (2006a) and Lind et al. (2009b) find a trend between $A(\text{Li})$ and T_{eff} along the SGB and the early RGB, roughly consistent with models (Richard et al. 2005, hereafter R05) that start with the BBNS $A(\text{Li})$ and include atomic diffusion moderated by some ad-hoc turbulent mixing that brings back to the surface some of the Li (and other elements) diffused below the convective envelope during the main sequence (MS) phase. González Hernández et al. (2009) have studied a sample of MS and SGB stars in the same cluster, and found $A(\text{Li})$ decreasing with decreasing T_{eff} in both groups of stars, with the SGB stars showing systematically higher values of $A(\text{Li})$ at a given T_{eff} . This pattern cannot be reproduced satisfactorily by any existing theoretical model starting with the BBNS value of $A(\text{Li})$.

It is relevant to highlight that the investigation of $A(\text{Li})$ in GCs needs some special care, because of the occurrence of chemical anomalies in the light elements. In fact, all the GCs studied so far exhibit large star-to-star variations of C, N, O, Na, Mg and Al and in particular anti-correlations between O and Na, and between Mg and Al (Carretta et al. 2009a,b). The widely accepted scenario to explain these patterns is that a second stellar generation was born in the cluster from the hydrogen-processed material ejected by the first population (Gratton et al. 2001). In this framework, Li could have a relevant role. A crucial point to recall is that the NeNa cycle, responsible for the pollution of the cluster gas, occurs at temperatures of $4\text{--}5 \cdot 10^7$ K, 20–30 times higher than the Li-burning temperature. Thus, unless the polluting stars are also able to produce Li, the second generation stars should be Li-poor with respect to the first one and Li-O correlations and Li-Na anticorrelations are expected. Previous investigations about this issue lead to conflicting conclusions: Pasquini et al. (2005) observed for the first time the Li-Na anticorrelation (and also the Li-O correlation) in 9 TO stars of NGC 6752 and a similar behaviour has been found also by Bonifacio et al. (2007) in 4 TO stars of 47 Tuc. In their sample of NGC 6397 TO stars, Lind et al. (2009b) detected 3 stars out of 100 with low Li and high Na abundances, suggesting a possible Li-Na anticorrelation, while all the other TO stars share the same Li abundance over a range of ~ 0.8 dex in $A(\text{Na})$. Recently, D’Orazi et al. (2010) and D’Orazi & Marino (2010, hereafter DM10) presented Li abundances in TO stars of 47 Tuc and RGB stars of M4, respectively. In both cases, first and second generation stars share the same Li abundance, regardless of the Na and O content, but with different star-to-star scatter between the two stellar groups.

In this paper, we present the Li abundance measured from high-resolution spectra of a sample of stars ranging from the TO to the RGB Bump in the GC M4. This is the first determination of Li content in the dwarf stars of this cluster. The Li content in the TO stars of M4 is then compared with the Li abundances measured in other GCs, in the field stars, and with the WMAP+BBNS predictions.

¹ Adopting different rates for the ${}^3\text{He}(\alpha,\gamma){}^7\text{Li}$ reaction, Steigman (2007) derived a slightly lower value, $A(\text{Li}) = 2.65$, still in disagreement with the *Spite Plateau*.

The behaviour of $A(\text{Li})$ as a function of $[\text{Fe}/\text{H}]$ is discussed in the light of stellar evolution models with and without atomic diffusion. Also, the Fe content along the entire evolutionary path is discussed and it is used to quantify the efficiency of atomic diffusion. Finally, we discuss the possible role of turbulent mixing in the theoretical models and the open questions related to the determination of the pristine Li abundance of M4.

2 OBSERVATIONAL DATA

This work is based on high-resolution spectroscopic observations of 87 stars in M4 performed with the GIRAFFE@FLAMES spectrograph mounted at VLT@ESO, within a project aimed to search for anomalous abundances in the BSS atmospheres (see Ferraro et al. 2006). All stars have been observed with the HR15N, HR18 and HR22 gratings that include the Li doublet at 6707.8 \AA , the H_α Balmer line and several Fe I lines. The spectral sample includes 51 TO/SGB stars and 36 giants up to the RGB Bump magnitude level. Target selection, reduction of the spectra and measurement of the radial velocities are discussed in Lovisi et al. (2010). The position of the targets in the $(V, V-I)$ colour-Magnitude Diagram (CMD) is shown in Fig. 1 (left panel). The Signal-to-Noise Ratio (SNR) around the Li line is ~ 50 -80 for dwarf stars and rises up to about 300 for the brightest RGB stars. The membership of all the targets has been confirmed by the combined information of proper motions, radial velocities and metallicities, as discussed in Lovisi et al. (2010). Only one target in our sample has been found to be in common with the list of binaries by Sommariva et al. (2009) and it was excluded from the analysis.

3 ANALYSIS

3.1 Atmospheric parameters for TO/SGB stars

Atmospherical parameters for SGB stars have been already presented in Lovisi et al. (2010). Here we briefly discuss in more details only the derivation of T_{eff} . Temperatures have been computed from a χ^2 minimization between the observed wings of the H_α Balmer line and a grid of synthetic spectra. Synthetic spectra have been computed by means of the SYNTHE code from a grid of 1D LTE plane-parallel model atmospheres, obtained with ATLAS9 code in its Linux version (Kurucz 1993a,b; Sbordone et al. 2004). Adopted model atmospheres are based on the NEW Opacity Distribution Functions described by Castelli & Kurucz (2003) without inclusion of the *approximate overshooting* and with α -enhancement abundance patterns of $[\alpha/\text{Fe}] = +0.4$ dex. For the modeling of the Balmer line, we adopted the self-resonance broadening theory by Ali & Griem (1965, 1966).

The dominant source of error for T_{eff} derived from the Balmer line is due to the residuals in flat-fielding and blaze function correction, that can introduce residual and spurious curvatures in the spectrum, afflicting the continuum placement. Such an effect is not easy to model, but in the fiber-fed GIRAFFE spectra it is less critical than in the slit

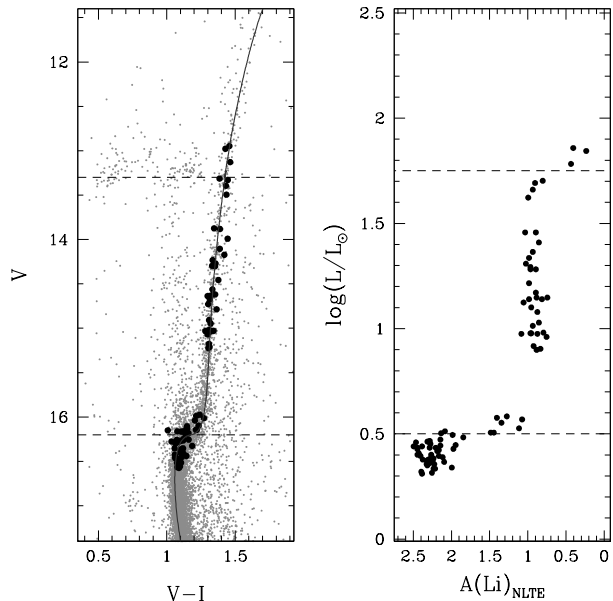


Figure 1. Left panel: colour-magnitude-diagram of M4 (gray dots) with spectroscopic targets marked as black filled circles. The solid line is the best-fit isochrone (see text for details). Right panel: behaviour of $A(\text{Li})$ as a function of luminosity. The two dashed horizontal lines denote the position of the two detected drops of $A(\text{Li})$ (see text for details).

spectra, since the flat-field is acquired through the same optical path used for the stellar spectra. In order to minimize this uncertainty, observed and synthetic spectra have been normalized by using the same continuum regions, typically $\pm 100 \text{ \AA}$ from the line centre.

In order to assess the internal error in the T_{eff} , we resorted to Monte Carlo simulations, similar to the procedures already adopted by Bonifacio et al. (2007) and Lind et al. (2008). The effect of the photon noise is quite small: we performed Monte Carlo simulations of 1000 synthetic spectra around the H_α line injecting Poissonian noise in order to reproduce the typical SNR of our spectra and we repeated the procedure to derive T_{eff} . We find that at SNR= 50 the error is of about 20 K, due to the large number of pixels used in the χ^2 minimization. A similar check has been performed to assess the impact of the adopted fitting windows. Finally, we attribute to our T_{eff} random errors of the order of 30-40 K. Other sources of uncertainties can affect the Balmer T_{eff} and considered as systematic errors, for instance the gravity dependence of H_α , the residual curvature in the flat-fielding, the adopted broadening theory and finite pixel-step in our spectra (see e.g. Bonifacio et al. 2007, for a detailed discussion of these source of errors). In particular, Bonifacio et al. (2007) and Sbordone et al. (2010) discussed the sensitivity of the H_α line to the gravity and found that it is important in the low metallicity regime ($[\text{Fe}/\text{H}] < -2.0$ dex), significantly lower than that of M4. For the TO stars we estimate a variation of only ~ 10 -20 K in T_{eff} for a variation of 0.5 in $\log g$, while for the coldest SGB stars such a sensitivity rises to ~ 40 K. Bearing in mind these sources of uncertainty and we conservatively attribute a typical, absolute error of 100 K to TO/SGB stars and of 150 K to the coldest SGB stars.

3.2 Atmospheric parameters for RGB stars

For RGB stars T_{eff} cannot be inferred with the procedure described above, since, the H_α wings are not sensitive enough to T_{eff} variations in cold stars. Some authors use the wings of H_α line to derive T_{eff} also for RGB stars, but it is worth noticing that this method, when applied to giant stars, is subject to very high uncertainties (of 300 K at least). For stars with $V < 15.3$, T_{eff} have been derived by projecting their position in the CMD on the best-fit isochrone. (left panel of Fig. 1, where the CMD is corrected for differential reddening). On the basis of the standard procedure (see for example Piotto et al. 1999), we estimate that the differential reddening is of the order of $\delta E(B-V) = 0.25$ in this cluster. The isochrone with appropriate metallicity ($Z = 0.004$, corresponding to $[Fe/H] = -1.01$ for $[\alpha/Fe] = +0.4$) and age (12 Gyr), has been selected from the BaSTI database² (Pietrinferni et al. 2006), and transformed into the observed plane by adopting $E(B-V) = 0.32$ and $(m-M)_0 = 11.30$, consistent with the results by Bedin et al. (2009).³ It is worth noticing that because of the high value of the extinction, we applied a reddening correction that takes into account the dependence of A_λ/A_V on the star surface gravity, T_{eff} and $[Fe/H]$. We did this by following the same procedure described in Bedin et al. (2009), adopting the extinction law of Cardelli et al. (1989), re-scaled to $R_V = 3.8$, which is the value measured in the direction of M4 (Hansen et al. 2004; Bedin et al. 2009).

The colour- T_{eff} transformations of the BaSTI database have been computed from the same model atmospheres adopted in our spectroscopic analysis. Hence such a T_{eff} scale is formally homogeneous with that adopted for the dwarf stars. Indeed the BaSTI isochrone T_{eff} scale well agrees with that derived from the H_α line for the TO/SGB stars: we find an average difference $T_{eff}^{BaSTI} - T_{eff}^{H_\alpha} = -28$ K ($\sigma = 126$ K) for stars with $V > 15.3$. Thus, no relevant systematic offset is introduced between the abundances computed for dwarf and giant stars (the effect of different T_{eff} scales on the derived abundances is discussed in Sect. 6.2). Taking into account the photometric error, the uncertainty in $E(B-V)$ and that arising from the differential reddening correction, we attribute a typical error of 100 K to T_{eff} of RGB stars.

Similarly to the dwarf stars (see Lovisi et al. 2010), the gravities have been obtained from the position of the stars in the CMD, and the microturbulent velocities have been derived spectroscopically, by erasing any trend between $A(Fe)$ and the equivalent width (EW). Main parameters, Li and Fe abundances for all the target are listed in Table 1, the complete version being available in electronic form.

3.3 Lithium

Li abundances have been measured by comparing the observed EWs of the Li I resonance doublet at 6707.8 \AA with the EW computed from a grid of synthetic spectra. A curve

of growth has been built for each star and we derived $A(Li)$ interpolating each curve at the observed EW value. Due to the small wavelength separation of the Li components, this line can be reasonably approximated with a single gaussian profile at the GIRAFFE resolution. EWs have been measured with our own FORTRAN procedure, that performs a gaussian fit on a spectral window selected interactively. The continuum level is traced locally by considering a region of $\sim 20 \text{ \AA}$ around the Li line, rejecting spikes, cosmic rays and spectral features with a σ -clipping algorithm and adopting as continuum level the peak of the flux distribution computed from the surviving points. As sanity check we performed an independent EW measurement by using the IRAF task *splot*, finding an average difference $EW_{IRAF} - EW_{fit} = -0.09 \text{ m\AA}$ with a dispersion $\sigma = 2.35 \text{ m\AA}$. Such a small difference is irrelevant to the purposes of this work.

Atomic data for the Li doublet, including its hyperfine structure and isotopic splitting (with $N(^6Li)/N(^7Li) = 8\%$), are from Yan & Drake (1995). Corrections for NLTE effects have been applied by interpolating the grid of Carlsson et al. (1994): derived NLTE corrections are quite small, of the order of 0.01 dex⁴.

The error in $A(Li)$ is computed by adding in quadrature the two main sources of uncertainty, namely the errors arising from T_{eff} and from the EW measurement. $A(Li)$ turns out to be very sensitive to the used T_{eff} , because Li is almost totally ionized. The typical error in T_{eff} (± 100 K) translates in an error in $A(Li)$ of ± 0.07 dex for TO/SGB stars and slightly higher (± 0.09 dex) for RGB stars. It is customary to estimate the error in EW measurement by using the Cayrel formula (Cayrel 1988). This gives ± 4 - 4.5 m\AA for TO/SGB stars and ± 1 - 2 m\AA for RGB stars, translating in $A(Li)$ errors of the order of ± 0.05 - 0.07 dex and of ± 0.01 - 0.02 dex, respectively. The Cayrel formula neglects the uncertainty due to the continuum location, that can have a relevant impact in spectra with low SNR. We estimated the continuum location uncertainty from the average spread of the residual spectrum around the Li line and performing several tests with different assumptions of the continuum level. Finally we derive an uncertainty of ± 0.10 dex for the TO/SGB stars with lowest SNR and a few hundredths of dex for the RGB stars. Other sources of errors (linked to gravity and microturbulent velocity) can be assumed to be negligible since they correspond to an error in $A(Li)$ of ± 0.01 dex each. Final absolute errors in $A(Li)$ range between ± 0.08 and ± 0.15 dex, according to the stellar evolutionary stage.

3.4 Iron

Our spectral dataset allows to measure the Fe abundance in both TO/SGB and RGB stars. In turn these measures can be used as tracers of the occurrence of atomic diffusion processes along the evolutionary path. Fe abundances for all the target stars have been derived from the EW measurement by using WIDTH code⁵ in its Linux version (Sbordone et al.

² <http://albione.oa-teramo.inaf.it/>

³ The adopted isochrone is calculated without atomic diffusion. Including atomic diffusion would change the age of the isochrone of about 1 Gyr but the T_{eff} -colour relation would be essentially unchanged.

⁴ Note that the adoption of the NLTE corrections of Lind et al. (2009a) would have a negligible (of about a few hundredths) impact on the Li abundances.

⁵ We have employed a version of the original code by R. L. Kurucz modified by F. Castelli, in order to use

Table 1. Identification numbers, coordinates, temperatures, gravities, EW of the Li line, A(Li) and [Fe/H] abundances, SNR around the Li line for the observed stars. A complete version of the table is available in electronic form.

ID	RA	Dec	T_{eff}	log g	EW(Li)	A(Li)	[Fe/H]	SNR
	(J2000)	(J2000)	(K)	(dex)	(mÅ)	(dex)	(dex)	
8460	245.9471429	-26.3749119	5000	2.8	22.7	0.96	-1.14	104
8777	245.9373405	-26.3613910	5150	3.2	11.8	0.79	-1.13	85
9156	245.9069486	-26.3438488	4950	2.7	20.9	0.85	-1.06	217
13282	245.7901731	-26.3909501	5850	3.9	39.5	2.11	-1.00	53
28007	245.8049983	-26.6687472	5100	3.0	13.6	0.81	-1.16	116
28890	245.8083640	-26.6339178	5850	3.8	30.5	1.98	-1.06	62
28999	245.7440673	-26.6298102	6000	4.0	34.4	2.16	-1.20	68
29074	245.8010945	-26.6273020	6150	3.9	34.8	2.28	-1.00	48
29411	245.7990049	-26.6149585	5500	3.7	15.9	1.34	-1.05	60
29643	245.7572145	-26.6058864	5800	3.8	40.3	2.08	-1.19	68
29729	245.7547183	-26.6022333	5950	3.9	46.8	2.28	-1.18	58
30167	245.7958060	-26.5866438	5950	3.8	35.6	2.14	-1.04	60
30475	245.7195282	-26.5759641	5100	3.0	12.0	0.74	-1.05	158
30922	245.7432036	-26.5602858	6050	4.0	33.1	2.18	-1.16	48

2004). We employed two different linelists for TO/SGB and RGB stars, in order to include only unblended transitions, by taking into account the different degree of blending and line strength between dwarf and giant stars. The number of Fe I lines is limited by the relatively small wavelength coverage of our spectra (we remark that the spectral regions sampled by the gratings HR18 and HR22 are strongly affected by deep telluric absorptions). Finally, we derived the abundance from ~ 6 -14 and ~ 18 -22 Fe I lines, for TO/SGB and RGB stars respectively. Atomic data are from the classical line compilation by Fuhr, Martin & Wiese (1988). As solar reference we adopted $A(Fe)_{\odot} = 7.5$ dex (Grevesse & Sauval 1998). The error estimate has been performed similarly to what we did for Li. Taking into account the typical uncertainty on the atmospheric parameters we estimate a systematic error of about ± 0.10 and ± 0.15 dex for SGB and RGB stars, respectively. Random error obtained from the Cayrel formula and the continuum level uncertainty ranges from ± 0.14 (for SGB) to ± 0.03 dex (for RGB stars).

4 EVOLUTION OF A(LI)

The right panel of Fig. 1 shows the behaviour of A(Li) as a function of luminosity for the observed targets. Luminosities have been derived from the best-fit BaSTI isochrone discussed above and according with the position of the star along the evolutionary sequences. The two horizontal dashed lines denote the magnitude and luminosity levels where two abrupt drops of A(Li) occur. Fig. 2 shows the values of A(Li) as a function of T_{eff} . We can describe the evolutionary behaviour of the Li abundance by identifying four regimes in Fig. 1 and 2:

- **TO** ($T_{eff} \geq 5900$ K; $\lg(L/L_{\odot}) < 0.5$): stars located at the TO level have an average $\langle A(Li) \rangle = 2.30 \pm 0.02$ dex

($\sigma = 0.10$). To check whether the distribution of Li abundances is consistent – given the observational random errors – with a uniform value $A(Li) = 2.30$, we performed the following test (see, e.g., an application of the same test to the analysis of initial He abundances in GCs and of GC ages by Cassisi et al. 2003; Chaboyer et al. 1996; Salaris & Weiss 2002). For each individual star we have calculated a set of synthetic Li abundances by randomly generating – using a Monte Carlo procedure – 10000 abundance values, according to a Gaussian distribution with mean value equal to $A(Li) = 2.30$, and σ equal to the empirical random abundance errors. As random errors we have considered the errors due to the EW measurements (as described in Sect. 3.3) and the random errors in the T_{eff} determination (as described in Sect. 3.1). This is repeated for all 35 TO stars, and the final 350000 synthetic values are combined to produce an “expected” distribution for the entire sample, in the assumption that the detected Li abundance dispersion is not intrinsic, but due to the individual errors, assumed Gaussian. The statistical F-test was then applied to determine if this “expected” distribution (well sampled by the extremely large number of elements), displays a variance that is statistically consistent with the observed distribution of 35 objects. As customary, we state that an intrinsic A(Li) range of values does exist if the probability P that the two distributions have different variance is larger than 95%.

We find a value of P below 90%, and therefore we can conclude that the observed dispersion is formally consistent with the random errors associated to the Li estimates of each star, and that our measurements provide a uniform Li abundance $A(Li) = 2.30 \pm 0.02$ for all objects with $T_{eff} \geq 5900$ K.

This result points toward a general homogeneity of the Li abundance in M4 stars, in contrast to the large star-to-star scatter observed in other clusters (as 47 Tuc and NGC 6752) that indicates an intrinsic dispersion in A(Li).

- **SGB** (5200 K $< T_{eff} < 5900$ K; $0.5 < \lg(L/L_{\odot}) < 0.6$): these stars are located along the SGB, from the TO to the base of the RGB. We found a decrease of A(Li) for increasing T_{eff} , with A(Li) ranging from 2.0 (in the hot SGB stars) to 0.9 dex (at the end of the SGB).

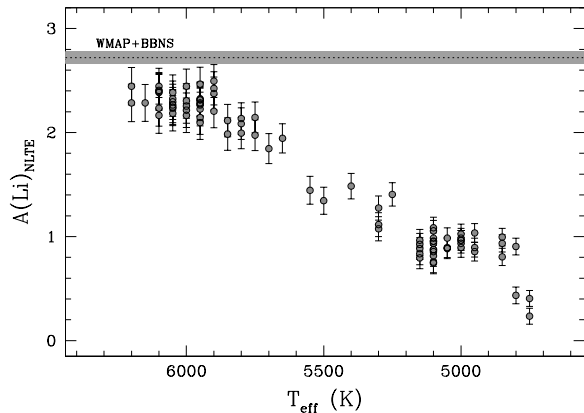


Figure 2. Behaviour of $A(\text{Li})$ as a function of T_{eff} for individual stars. The error bars include both random and systematic errors. The dotted line denotes the WMAP+BBNS value of $A(\text{Li})$ computed by Cyburt et al. (2008) and the grey area the corresponding uncertainty.

- **lower-RGB** ($4800 \text{ K} < T_{\text{eff}} < 5200 \text{ K}$; $0.9 < \lg(L/L_{\odot}) < 1.7$): stars in this luminosity range, corresponding to the portion of the RGB fainter than the RGB Bump (that occurs for this age and metallicity at $\lg(L/L_{\odot})=1.73$), share the same abundance of Li, defining a plateau $\langle A(\text{Li}) \rangle = 0.92 \pm 0.01 \text{ dex}$ ($\sigma = 0.08$).

- **upper-RGB** ($T_{\text{eff}} < 4800 \text{ K} - \lg(L/L_{\odot}) > 1.7$): these stars are brighter than the RGB Bump and display a sudden drop of $A(\text{Li})$, reaching $A(\text{Li}) \sim 0.23 \text{ dex}$.

We remark that M4 is the second GC studied so far, after NGC 6397 (Lind et al. 2009b), where $A(\text{Li})$ has been measured along the TO-SGB-RGB sequence: in both clusters two drops of $A(\text{Li})$ have been clearly detected, consistent with the pattern already seen in Halo stars (Gratton et al. 2000). These drops can be associated with two distinct mixing episodes:

(i) the canonical mixing episode called *First Dredge-Up* that occurs when the convective envelope reaches inner regions where Li has been destroyed through the nuclear reaction ${}^7\text{Li}(p,\alpha){}^4\text{He}$; this produces a drop of $A(\text{Li})$ by a factor ~ 15 along the SGB;

(ii) the extra-mixing episode after the RGB Bump, that occurs when the outward moving H-burning shell reaches the discontinuity in the H-profile left over by the convective envelope at its maximum penetration (see e.g. Charbonnel & Lagarde 2010). The stars at $V \sim 13.5$ (where the RGB Bump is located, see e.g. Ferraro et al. 1999) share the same abundance of the fainter RGB stars, while the 3 RGB stars above this luminosity display a drastic decrease of $A(\text{Li})$. When the mean molecular weight barrier is removed after the RGB Bump, the surviving surface Li is destroyed and the stars exhibit $A(\text{Li})$ approaching zero.

The Li abundance measured in M4 TO stars, $A(\text{Li})=2.30 \text{ dex}$, is in agreement with what found in all other GCs investigated so far (Fig. 3). The metal-

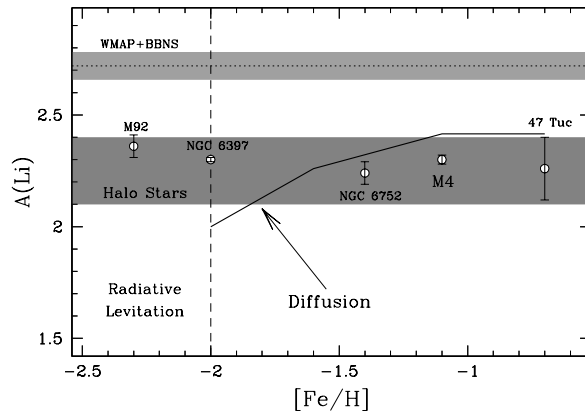


Figure 3. $A(\text{Li})$ mean values for TO stars in the GCs studied so far, as a function of the initial cluster iron abundance measured from the RGB stars. Errorbars indicate the dispersion around the mean, normalized to the root mean square of the number of used stars. The dark grey area displays the range of values obtained for Halo stars by different recent investigations (Bonifacio & Molaro 1997; Charbonnel & Primas 2005; Asplund et al. 2006; Bonifacio et al. 2007; Aoki et al. 2009). The solid line displays the theoretical prediction for the value of $A(\text{Li})$ in TO stars for an age of 11-12 Gyr, in case atomic diffusion is fully efficient, starting from an initial WMAP+BBNS value $A(\text{Li})=2.72$. The vertical dashed line shows the boundary for the radiative levitation to start affecting appreciably the photospheric chemical abundances of Li (see Sect. 8 for details). The primordial $A(\text{Li})$ provided by WMAP+BBNS calculations and the associated uncertainty is also displayed (light grey region).

poor ($[\text{Fe}/\text{H}]=-2.3 \text{ dex}$) GC M92 shows a mean value of $A(\text{Li})=2.36 \pm 0.05 \text{ dex}$, $\sigma = 0.18$, (Bonifacio 2002). For NGC 6397 ($[\text{Fe}/\text{H}]=-2.0 \text{ dex}$) different studies point toward $A(\text{Li})$ between 2.25 ± 0.01 (Lind et al. 2009b) and $2.30 \pm 0.01 \text{ dex}$ (González Hernández et al. 2009) in stars along the MS or around the TO. The value of $A(\text{Li})$ in 9 TO stars of NGC 6752 ($[\text{Fe}/\text{H}]=-1.4 \text{ dex}$) has been measured by Pasquini et al. (2005) who found $A(\text{Li})=2.24 \pm 0.05 \text{ dex}$ ($\sigma=0.15$). Finally, the metal-rich cluster 47 Tuc (D’Orazi et al. 2010) shows a similar mean abundance, but with a large star-to-star scatter, $A(\text{Li})=2.26 \pm 0.14 \text{ dex}$ ($\sigma=1.38$).

Even if small offsets can be present between these Li determinations (because of the different temperature scales and adopted NLTE corrections), all these measurements are consistent each other and with the *Spite Plateau* detected in the Halo dwarf stars (grey region). Hence, we confirm for M4 the Li content discrepancy with respect to the WMAP+BBNS results, already detected in the field stars and in other GCs.

5 EVOLUTION OF $[\text{Fe}/\text{H}]$

Fig. 4 shows the estimated $[\text{Fe}/\text{H}]$ as a function of T_{eff} for the individual stars in our sample. The iron abundance

does not show any systematic trends with the temperature. By taking into account the entire sample, the average Fe abundance for M4 turns out to be $[\text{Fe}/\text{H}] = -1.10 \pm 0.01$ dex ($\sigma = 0.07$). This value basically agrees with previous spectroscopic analyses. Ivans et al. (1999) derived an average iron content $[\text{Fe}/\text{H}] = -1.18 \pm 0.01$ dex, Marino et al. (2008) obtained $[\text{Fe}/\text{H}] = -1.07 \pm 0.01$ dex, Carretta et al. (2009c) found a value $[\text{Fe}/\text{H}] = -1.18 \pm 0.02$ dex. Taking into account the adopted solar reference values, the absolute differences between our Fe determinations and the previous ones are of $+0.06$, -0.01 and $+0.04$ dex, respectively. By dividing the sample in 3 groups, e.g. considering separately 35 TO stars, 16 SGB stars and 36 RGB stars, the derived average Fe abundances are $[\text{Fe}/\text{H}] = -1.08 \pm 0.01$ ($\sigma = 0.07$), -1.13 ± 0.03 ($\sigma = 0.07$) and -1.11 ± 0.01 ($\sigma = 0.07$), respectively. Hence, no evident trend is detected between dwarf and giant stars. A F-test analogous to the one described for the TO sample has been performed on the $[\text{Fe}/\text{H}]$ values of our whole sample of M4 stars, and has provided – as expected – no statistically significant indication of an intrinsic spread.

Note that this analysis does not include any correction for the departures from LTE, due to the lack of NLTE corrections for individual Fe I lines at the metallicity of M4. Moreover, the precise order of magnitude of NLTE corrections for Fe lines is not well constrained, because some assumptions must be introduced (for instance the factor S_H needed to correct the H I collisional cross-sections derived by the formula by Drawin (1968) and the accuracy and completeness of the adopted model Fe atom). Although the departures from LTE are more critical at lower metallicities, we have tried to use the corrections computed by Gratton et al. (1999) for a representative high excitation Fe I transition⁶, for an overall metallicity $[\text{M}/\text{H}] = -1.0$ dex. These NLTE–LTE corrections are positive and quite small (~ 0.05 dex for dwarfs and ~ 0.03 dex for giant stars) and, if applied, they do not change the observed trend and are not capable to introduce a systematic offset in $[\text{Fe}/\text{H}]$ between TO/SGB and RGB stars.

6 SANITY CHECKS

6.1 Median spectra

To reduce the error sources and strengthen our result about the SGB stars (that have the lowest SNR), we averaged their spectra according to their individual T_{eff} . We obtained five spectra with enhanced SNR (~ 150 around the Li line) and repeated the entire analysis for each of them: normalization of the spectrum, re-computation of T_{eff} by fitting H_α wings and measurements of EWs for Li and Fe. The resulting new set of T_{eff} well resembles the average of the single spectra values within ~ 40 K, confirming the reliability of the individual T_{eff} . Also, A(Li) and $[\text{Fe}/\text{H}]$ measured in these median spectra agree within few hundredths of dex with the average Li and Fe abundances computed from the individual stars.

⁶ Note that the majority of the adopted Fe I lines in our analysis has excitation potential > 3 eV.

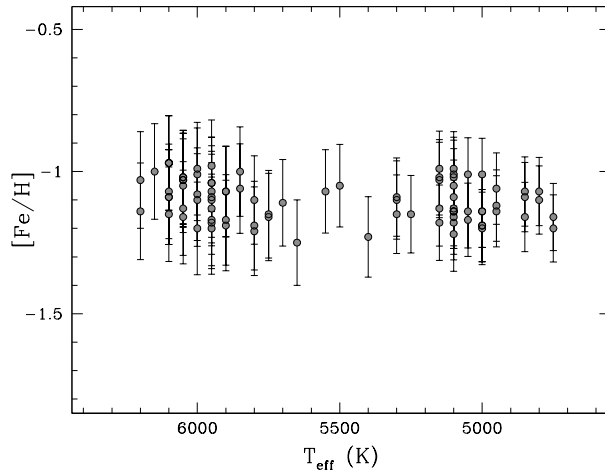


Figure 4. Behaviour of $[\text{Fe}/\text{H}]$ as a function of T_{eff} for the individual stars in our sample. Errorbars include random and systematic errors.

6.2 The impact of different T_{eff} scales

The Li abundance shows a plateau for temperatures larger than $T_{\text{eff}} = 5900$ K (see Fig.2). The reliability of this trend is crucial, because stellar evolutionary models including pure atomic diffusion predict an increase of A(Li) before the dilution due to the *First Dredge-Up* (see e.g. the discussion in Salaris & Weiss 2001).

The most relevant source of error in the A(Li) determination is the assumption of the T_{eff} scale. We therefore repeated the analysis by adopting two different photometric T_{eff} scales, derived by means of the most recent $(V - I)_0 - T_{\text{eff}}$ relations by González Hernández & Bonifacio (2009, GHB09) and Casagrande et al. (2010, C10), both based on the InfraRed Flux Method (IRFM). We remark that these T_{eff} scales are independent of the T_{eff} derived by the H_α line and affected by different source of errors. In particular, T_{eff} inferred by IRFM are largely insensitive to uncertainties in model atmospheres (i.e. the adopted line broadening recipe, the assumption of 1-dimensional geometry) at variance with those derived from the H_α line, but they are affected by uncertainties on the photometry, absolute and differential reddening, photometric calibration and so on. We have derived $(V - I)_0$ colours for our stars from the WFI photometry, corrected for differential reddening effects (see Sect. 3.2). By adopting the GHB09 calibration, we find an average difference $T_{\text{eff}}^{\text{GHB09}} - T_{\text{eff}}^{\text{H}\alpha} = -77$ K ($\sigma = 125$ K). Similarly, the temperatures computed by the C10 calibration provide a mean difference $T_{\text{eff}}^{\text{C10}} - T_{\text{eff}}^{\text{H}\alpha} = -29$ K ($\sigma = 123$ K). These mean differences are small in absolute terms and also much smaller than the dispersion around their mean values. We therefore conclude that no significant difference is found between the T_{eff} scales obtained from the Balmer line and from the IRFM. This finding reduces the major disagreement between previous generations of theoretical $(V - I)_0 - T_{\text{eff}}$ transformations and IRFM calibrations (see the extensive discussion by Weiss & Salaris 1999).

We have however re-analyzed our stars by employing

also these two T_{eff} scales, re-computing both gravities and microturbulent velocities. The adoption of IRFM T_{eff} scales does not change the global behaviour of our abundances, both Li and Fe. In particular, the iron content remains consistent between TO and RGB stars, without systematic offset between the different group of stars. Variations of about ~ -0.05 dex or less are obtained for the average $A(\text{Li})$ of TO stars.

These checks further reinforce the conclusion that the observed behaviour of $A(\text{Li})$ and $[\text{Fe}/\text{H}]$ as a function of T_{eff} is not an artifact due to an incorrect T_{eff} scale.

6.3 Comparison with D’Orazi & Marino (2010)

The only other sample of Li abundance in M4 stars available to date concerns 104 RGB stars discussed by DM10. There is a small overlap between the 2 samples, with only 5 RGB stars in common. The agreement with their atmospheric parameters is satisfactory, despite different methodologies have been applied (i.e., for T_{eff} we use the comparison with the BaSTI isochrone, while DM10 relies on the excitation equilibrium method). Our T_{eff} values are higher by +36 K ($\sigma = 22$ K) on average, and also the gravities show very small differences (of the order of 0.2 dex). The mean difference between the iron abundances of these 5 targets is of only -0.04 dex ($\sigma = 0.06$ dex), including also a small offset in the solar zero-point. Although atmospheric parameters and iron abundances are fully consistent between the two studies, a large (~ 0.4 dex) difference is revealed in the Li content of 3 stars, while for the other 2 objects DM10 provide $A(\text{Li})$ close to zero, lower than our measures. The discrepancies are not attributable to the quoted measurement errors, nor to the difference in T_{eff} (which leads to a difference in $A(\text{Li})$ of ~ 0.02 dex only). Fig. 5 shows the Li line in our spectra for the five stars in common, compared with synthetic spectra computed with our abundances (solid grey curve) and with those by DM10 (dotted grey curve). Note that for the 2 stars with $A(\text{Li}) \sim 0$ in DM10, the differences are consistent with the different SNR of the spectra, because in their spectra (with typical SNR 50-100) such weak Li lines are hidden in the noise envelope. For the other 3 stars the discrepancy is more critical.

DM10 have employed ATLAS9 model atmospheres computed with the option of *approximate overshooting*. As pointed out by Molaro, Bonifacio & Primas (1995) and Bonifacio et al. (2009), the temperature stratification of ATLAS9 model atmospheres with and without *approximate overshooting* can be very different in the optical depth range $-1 < \lg(\tau) < 1$, where the bulk of the weak/moderated lines is formed (including the Li line adopted in this work). We computed some ATLAS9 model atmospheres with *approximate overshooting* and compared the synthetic Li line profile in the two cases. At the metallicity of M4, the difference between the thermal structures of the two models is less severe than at lower metallicities (as those investigated by Bonifacio et al. 2009), and the adoption of the ATLAS9 models with *approximate overshooting* leads to an increase of the Li abundance smaller than 0.1 dex.

As a sanity check, we apply our procedure to the GIRAFFE dataset of NGC 6397 stars studied by Lind et al. (2009b). We retrieved the reduced data from the GIRAFFE

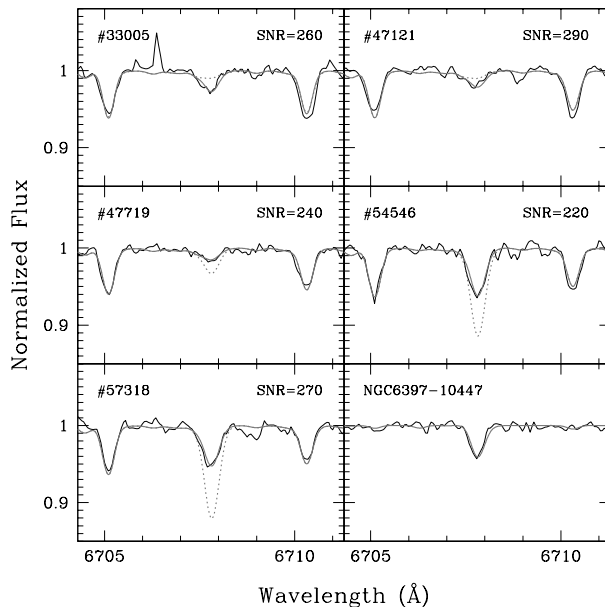


Figure 5. Portions of the GIRAFFE spectra (solid black) around the Li line for 5 RGB stars in common with DM10. Solid grey lines show synthetic spectra computed with our Li abundances, and dotted grey lines display spectra computed with Li abundances from DM10. The bottom-right panel shows the Li line in the spectrum of star 10447 belonging to NGC 6397, from the dataset by Lind et al. (2009a), compared to a synthetic spectrum computed with their atmospheric parameters and Li abundance $A(\text{Li})=1.04$ (see text for details).

Archive maintained at the Paris Observatory ⁷ and derived $A(\text{Li})$ for a sub-sample of their targets by using our procedure and their atmospheric parameters and EWs. Differences of a few hundredths of dex with respect to the derived $A(\text{Li})$ by Lind et al. (2009b) have been found. The bottom-right panel of Fig.5 shows a RGB star from the sample by Lind et al. (2009b), in comparison with a synthetic spectra computed with their atmospheric parameters and $A(\text{Li})$. From this test, we exclude any relevant systematic offset in our procedure to infer the Li abundance. As a further check, we redetermined the EWs of the Li line in a number of Lind et al. (2009b) stars, finding negligible differences. This confirms the reliability of our method to measure the EWs. These two tests give further support to the correctness of our $A(\text{Li})$ values for the RGB stars, but the discrepancy with DM10 remains unexplained and we postpone this issue to future investigations.

Finally, we note that if our sample was affected by a systematic underestimate of $\sim 0.3-0.4$ dex for both RGB and TO stars, we would obtain $A(\text{Li}) \sim 2.7$ dex at the TO of M4, a value much higher than the $A(\text{Li})$ measurements along the *Spite Plateau* and in general higher than all the Li measurements in Pop II stars of the last three decades.

⁷ <http://giraffe-archive.obspm.fr/>

7 LI ABUNDANCE IN FIRST AND SECOND GENERATION STARS

As already mentioned in Section 1, the current interpretation of the anticorrelations observed in the GCs, involves a first generation of stars with efficient CNO, NeNa, and MgAl cycles in their interiors, whose chemically processed matter is transported to the surface, and ejected in the existing interstellar medium through mass loss processes. A second generation of stars is then formed out of this polluted matter, so that nowadays individual GCs are populated by a combination of first and second generation stars. The nature of this polluting first generation stars is still debated, with two competing candidates: intermediate-mass asymptotic giant branch (AGB) stars (Ventura & D’Antona 2009) or fast rotating massive stars (Decressin et al. 2007). In both cases Li is expected to be depleted, since the NeNa cycle occurs at temperatures higher than that of Li burning. However, if AGB stars are responsible for intracluster pollution, they may have also produced Li, through the Cameron-Fowler mechanism (Cameron & Fowler 1971), so that the surface $A(\text{Li})$ may be able to increase to values similar to the initial abundances. Thus, it is crucial to compare the Li abundance in first and second generation stars, bearing in mind that only the former should be born from a gas with the cosmological $A(\text{Li})$. To this purpose, we study the behaviour of $A(\text{Li})$ as a function of $[\text{O}/\text{Fe}]$. The $[\text{O}/\text{Fe}]$ abundance ratios have been derived by Lovisi et al. (2010) by measuring the permitted O I triplet at 7771-74 Å. Unfortunately, our dataset does not include Na transitions, usually adopted to well separate the two populations (see Lind et al. 2009b; D’Orazi et al. 2010, hereafter DM10), because the choice of the setups has been done for different purposes (see Lovisi et al. 2010).

Fig. 6 shows the distribution of TO and RGB stars (excluding the stars located along the two Li drops, see Fig. 1) in the $[\text{O}/\text{Fe}]$ - $A(\text{Li})$ plane. For both dwarf and giant stars, the Li abundance does not show any correlation with $[\text{O}/\text{Fe}]$, similar to what found in 47 Tuc (D’Orazi et al. 2010) and in M4 by DM10. Measuring the Spearman rank coefficient, we find $C_S = 0.05$ and 0.06 for dwarf and giant stars, respectively. Such a test confirms the lack of correlation between Li and O content.

Hence, the Li abundance appears to be very similar among first and second generation stars. Adopting as boundary between the two populations the median value of the oxygen distribution ($[\text{O}/\text{Fe}] \sim 0.30$ dex), we find very similar average $A(\text{Li})$ values, both for dwarf and giant stars. This finding points out that Li production occurs in this cluster.

In fact, if the progenitors of second generation stars are massive objects, they have destroyed their original Li content in their envelopes, whereas if AGB stars are responsible for intracluster pollution, they may have produced Li, through the Cameron-Fowler mechanism (Cameron & Fowler 1971), so that the surface $A(\text{Li})$ may be able to increase to values similar to the initial abundances. On the other hand, a point to recall is that the Cameron-Fowler mechanism to produce Li needs to some fine-tuning. The entire envelope of the AGB stars where Li has been produced must be ejected before the newly formed Li is destroyed. The uniformity of the $A(\text{Li})$ values around the TO and along the lower RGB points somewhat to Li produc-

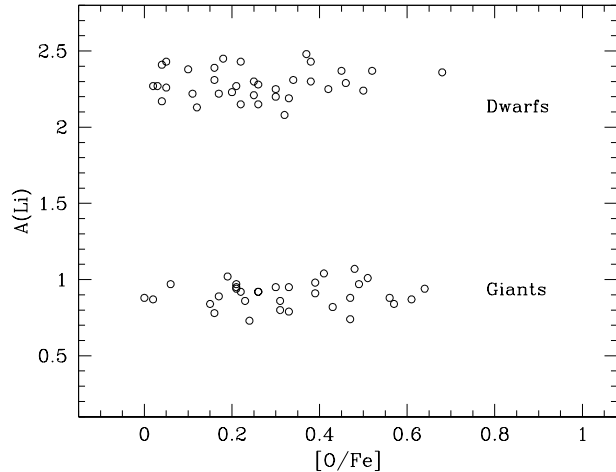


Figure 6. Behaviour of $A(\text{Li})$ as a function of $[\text{O}/\text{Fe}]$ for the stars of M4, excluding those located along the two Li drops (see Fig. 1).

tion in the polluters, as already discussed by DM10. In fact, since our sample of stars at a given T_{eff} contains a random mixture of stars belonging to both first and second generations, if the polluters destroy Li we would expect an intrinsic spread in $A(\text{Li})$. Conversely, if the polluters produce Li, a quite fine tuned scenario is required to achieve a uniform Li abundance for both first and second generations of stars in M4. In any case, several uncertainties (as the mass-loss rates and the Li yields) dramatically affect these kind of models.

8 THEORETICAL MODELS

To compare our measured Li and Fe abundances with the results from theoretical stellar evolution models – with and without including the effect of atomic diffusion – we have employed the stellar evolution code described in Pietrinferni et al. (2006). More in detail, we have considered an initial chemical composition with $Y = 0.25$, $[\text{Fe}/\text{H}] = -1.1$, and the same α -enhanced metal mixture as in Pietrinferni et al. (2006) and Salaris & Weiss (2001), with an average $[\alpha/\text{Fe}] = +0.4$ dex and with initial $A(\text{Li}) = 2.72$, corresponding to the WMAP+BBNS Li prediction. We have then computed the evolution of models with masses of the order of 0.85 - $0.89 M_{\odot}$ and TO age equal to 12 Gyr (for models without diffusion) and 11 Gyr (for models with diffusion). These objects are assumed to be the counterpart of stars currently evolving along the SGB and RGB of the cluster. The evolutionary sequences were computed starting from the pre-MS phase, until they reached $T_{eff} \sim 4700$ K along the RGB, i.e. below the lower T_{eff} limit of our observed stars.

Diffusion was included by solving the Burgers equations for a multicomponent fluid following Thoul, Bahcall, & Loeb (1994), and we considered explicitly the evolution of H, He, Li, C, N, O, and Fe abundances. The other elements have been assumed to diffuse like Fe. Our calculations account for the effects of temperature,

gravity and molecular weight gradients, while radiative levitation is not included.

As for the computation of the radiative opacity, given that for this metallicity all heavy elements are approximately equally diffused, the abundance ratios are not significantly affected, and the effects on the stellar opacity are accounted by interpolating among α -enhanced opacity tables of different Z . Superadiabatic convection is treated according to the mixing length formalism of Cox & Giuli (1968). The value of the mixing length has been chosen from a solar model calibration (see e.g. Pietrinferni et al. 2006). Finally, the rates for the Li destruction reactions are taken from the NACRE compilation (Angulo et al. 1999).

We remark that the only element transport mechanisms accounted for in our models are convection (with boundaries fixed by the Schwarzschild criterion and no overshooting) and atomic diffusion. No additional mixing process able to operate in RGB stars brighter than the RGB bump, or turbulent mixing that moderate the effect of atomic diffusion are included.

Given that our analysis focuses on the theoretical interpretation of the observed Li and Fe abundances, it is important to assess whether neglecting the radiative levitation – that tends to counteract the effect of temperature, gravity and molecular weight gradients – can affect our conclusions. Regarding the predicted surface Li abundances, Fig. 3 of Richard et al. (2002) and Figs 3 and 4 of Korn et al. (2006b) show that for metallicities above $[\text{Fe}/\text{H}] \sim -2$ the effect of neglecting radiative levitation is negligible.

As for the surface Fe abundances, the inclusion of radiative levitation at metallicities above $[\text{Fe}/\text{H}] \sim -1.3$ causes only small changes that do not affect any of the conclusions of our study. To give a quantitative example, we calculated a $[\text{Fe}/\text{H}] = -1.61$, 12 Gyr isochrone, and compared the surface $[\text{Fe}/\text{H}]$ values with the corresponding predictions in Fig. 9 of Richard et al. (2002), that include also the effect of radiative levitation. We find a depletion of $[\text{Fe}/\text{H}]$ close to the TO ($T_{\text{eff}} \sim 6300$ K) of 0.35 dex, compared to ~ 0.30 dex from Richard et al. (2002) results. Around the TO ($T_{\text{eff}} \sim 6200$ K) of a $[\text{Fe}/\text{H}] = -1.31$, 12 Gyr isochrone we find a $[\text{Fe}/\text{H}]$ depletion by 0.27 dex, compared to ~ 0.25 dex from the corresponding Richard et al. (2002) isochrone.

9 DISCUSSION

This section presents a detailed comparison between our Li abundance measurements and theoretical models, with the aim to assess the consistency between the initial $A(\text{Li})$ for M4 stars and the WMAP+BBNS value.

9.1 Comparison with the theory: the role of the diffusion

From the discussion in Sect. 4 it is clear that also M4 exhibits the discrepancy between the $A(\text{Li})$ value measured at the TO and the WMAP+BBNS estimate. We first investigate the role played by the atomic diffusion, that has been suggested by other authors as a possible solution to the problem, at least in case of NGC 6397 (Korn et al. 2006a). Fig. 7 and 8 display the comparison between the measured surface

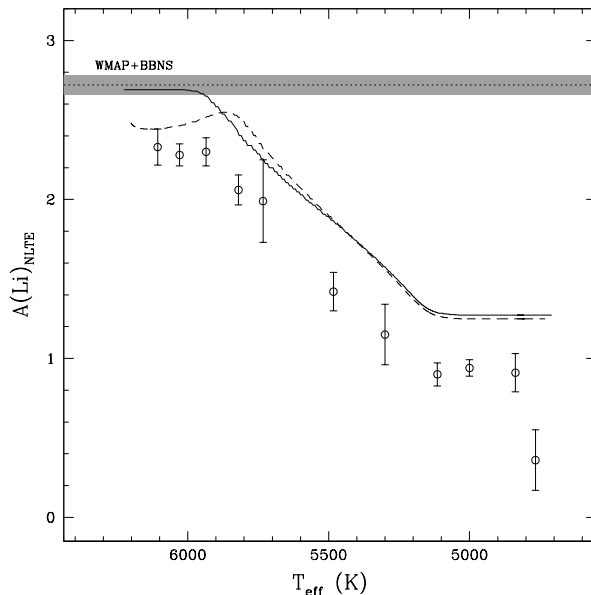


Figure 7. Behaviour of $A(\text{Li})$ as a function of T_{eff} for our sample of stars grouped in eleven T_{eff} bins. The curves indicate the theoretical predictions with (dashed line) and without (solid line) diffusion. Dotted line denote the primordial $A(\text{Li})$ computed by Cyburt et al. (2008) and the grey area the corresponding uncertainty.

Li and Fe abundances (grouped in 100–150 K wide temperature bins only for sake of clarity ⁸) and the predictions of evolutionary models with and without atomic diffusion, from the TO to the lowest temperature limit of our sample. For sake of comparison, we also plot the WMAP+BBNS $A(\text{Li})$ value used in the initial composition of our models, and the related uncertainty. The value $A(\text{Li})$ at the TO in the calculations without diffusion is very similar to the initial value (lower by only 0.03 dex) because the pre-MS Li depletion at these metallicities and for the TO mass of M4 is negligible. This value of $A(\text{Li})$ stays constant (within the uncertainties) from the TO to a point along the SGB with $T_{\text{eff}} \sim 5900$ – 6000 K; below this temperature, the surface Li abundance drops steadily, for the inward extending base of the convective envelope is reaching increasingly hotter layers where Li has been burned. This surface depletion ends when the convective envelope attains its maximum depth at the beginning of the RGB.

In the model with diffusion, the surface Li around the TO is depleted by about 0.2–0.25 dex, in agreement with results by Richard et al. (2002, see their Fig. 9). With decreasing temperature along the SGB, the surface $A(\text{Li})$ starts to rise again due to deepening of the convective region, that returns to the surface some of the Li diffused outside the envelope along the MS. $A(\text{Li})$ reaches a peak when $T_{\text{eff}} \sim 5800$ – 5900 K, with an abundance within ~ 0.1 dex from the initial one. Moving to lower effective temperatures, the surface Li abundance starts to drop, because the convective envelope reaches regions where Li had been burned due to the higher

⁸ Note that the adoption of different binning steps does not change dramatically the results.

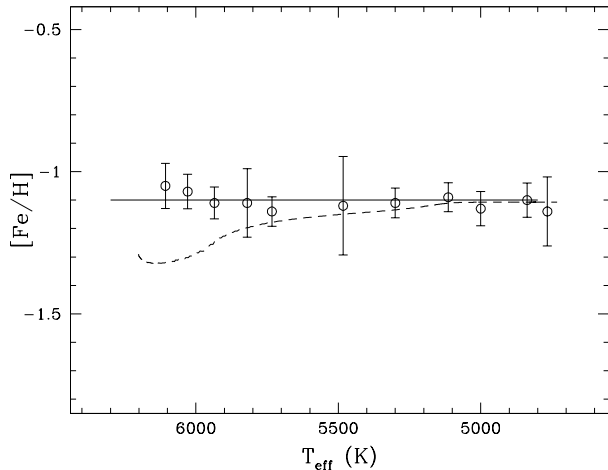


Figure 8. Behaviour of $[\text{Fe}/\text{H}]$ as a function of T_{eff} for our sample of stars grouped in eleven T_{eff} bins (same binning of Fig. 7). The curves indicate the theoretical predictions with (dashed line) and without (solid line) diffusion.

temperatures of the stellar matter. As for the case without diffusion, surface depletion ends when the convective envelope attains its maximum inward extension.

Fig. 9 helps to better clarify this behaviour. The Li abundance profile inside a model representing the cluster TO stars is displayed as a function of the temperature, for calculations with and without diffusion. The model calculated without diffusion displays a constant $A(\text{Li})$ even beyond the convective envelope boundary, located at $\log(T) \sim 6.02$, down to layers where the temperature is high enough to burn Li. The very small (~ 0.03 dex) difference with respect to the initial value is due to Li-burning during the pre-MS stage. When the model evolves along the SGB, convection deepens. As long as the bottom of the convective envelope stays within the temperature range where the Li profile is constant, the surface abundance does not change. When the base of the convective envelope reaches $\log(T) = 6.3-6.35$, it engulfs Li-depleted layers and the surface $A(\text{Li})$ decreases steadily, until the envelope reaches its maximum extension at the end of the SGB phase. At this point the surface depletion ceases and the surface $A(\text{Li})$ predicted by the models stays constant during the following RGB evolution. In case of models with diffusion, below the base of the convective envelope $A(\text{Li})$ first increases, due to the accumulation of Li diffused below the convection zone during the MS. When T reaches the Li-burning temperature, $A(\text{Li})$ drops fast, as in the model without diffusion. Along the SGB evolution, the base of the convective region engulfs first the layers with increased $A(\text{Li})$, and this causes the observed surface abundance increase after the TO. When convection goes deeper than $\log(T) = 6.3-6.35$, the behaviour of the surface $A(\text{Li})$ becomes similar to the case without diffusion. It is important to notice that the observed constant value of $A(\text{Li})$ along the RGB – before the RGB bump mixing episode that is

not accounted for by the models – provides an additional constraint on the Li content at the TO, that is rarely considered in the majority of the chemical analyses. In fact, given that the maximum depth of the convective envelope attained at the base of the RGB is independent of the exact value of the initial Li abundance, the predicted $A(\text{Li})$ along the lower RGB is determined by the internal Li abundance profile at the TO.

As for the trend of $[\text{Fe}/\text{H}]$ with T_{eff} , the model without diffusion displays essentially a constant $[\text{Fe}/\text{H}]$ along the whole evolution, equal to the initial value (the effect of the *First Dredge-Up*, that decreases slightly the surface H-abundance, is negligible). Instead the model with diffusion has an abundance lower by 0.21 dex around the TO, due to the diffusion of Fe below the convective envelope during the MS phase. Along the SGB $[\text{Fe}/\text{H}]$ increases steadily, for the increasing depth of the surface convective region brings back to the surface most of the Fe previously diffused from the convective envelope. When the model reaches the RGB, the surface Fe abundance is only very slightly lower than the initial value, and stays constant thereafter. We estimate that the T_{eff} of the TO stars should be increased by at least 300 K in order to lower the estimated iron abundance to values consistent with the predictions of models including atomic diffusion, while keeping the same T_{eff} for the RGB stars. However, the resulting T_{eff} for the TO stars would be incompatible with the T_{eff} of theoretical isochrones, with or without diffusion.

Some considerations can be drawn from the comparison between the observations and the theoretical models:

- (1) we measure a uniform value of $[\text{Fe}/\text{H}]$ along all the evolutionary sequences, that is reproduced by the model without diffusion. Taken at face value, this suggests that a process able to inhibit atomic diffusion from the convective envelope must be at work in the M4 stars;
- (2) both the models with and without diffusion, that start from a WMAP+BBNS initial Li abundance, predict $A(\text{Li})$ for TO stars higher than our measurements in M4 (see Fig. 7);
- (3) there is no observational evidence within the current observational errors for the $A(\text{Li})$ peak before the SGB drop, predicted by the models with atomic diffusion (see Fig. 7);
- (4) both the theoretical curves in Fig. 7 match reasonably well the value of T_{eff} (~ 5900 K) where Li dilution due to the penetration of the convective envelope starts, and the temperature ($T_{\text{eff}} \sim 5200-5300$ K) where the *First Dredge-Up* ends. However, a clear offset in $A(\text{Li})$ is recognized. In fact, the models predict $A(\text{Li}) \sim 0.30$ dex higher than that observed among the SGB and RGB stars. This offset cannot be erased by adopting different T_{eff} scales (see Sect. 6.2). It is interesting to note that also in NGC 6397 (Korn et al. 2006a, see their Fig. 1), the Li abundance among the RGB stars is lower than that predicted by the models tuned to fit the TO and SGB data (R05) by ~ 0.2 dex (despite this vertical offset has been not discussed by the authors).

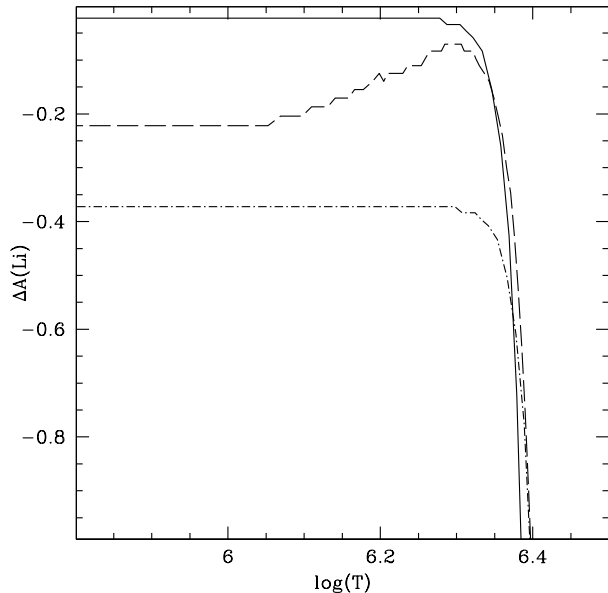


Figure 9. Li abundance profile (in terms of the difference with respect to the initial value adopted in the calculations) as a function of temperature, for a model corresponding to M4 TO stars, including (dashed line) and neglecting (solid line) diffusion. The dot-dashed line denotes the abundance profile needed to reproduce the measurements of $A(\text{Li})$ in the cluster (see Fig. 10).

9.2 Comparison with the theory: the role of the turbulence

A quite debated route to solve the discrepancy between the WMAP+BBNS Li abundance and the measurements along the *Spite Plateau* is to assume that, besides atomic diffusion, a turbulent mixing process occurring below the convective region is at work, partially or totally counteracting the effect of diffusion from the envelope. The models developed by R05 account for atomic diffusion (including radiative levitation) plus an *ad hoc* parametrization of turbulent mixing that limits the settling of Li (and other metals), and at the same time does not transport matter into the convective envelope where Li has been burned by nuclear reactions. In particular, the models computed with reference temperature $\log(T)=6.0$ ⁹ allow Korn et al. (2006a) to reproduce the observed TO and SGB $A(\text{Li})$ measurements in NGC 6397, starting from a primordial $A(\text{Li})=2.54$ (lower than more recent estimates from WMAP+BBNS calculations) and the small $[\text{Fe}/\text{H}]$ difference (~ 0.17 dex) they measure between TO and RGB stars.

Let's consider the internal Li profile for the model calculated with diffusion, as that displayed in Fig. 9. Any turbulence that brings back into the convective envelope some of the Li accumulated around $\log(T)=6.3$ will increase the surface $A(\text{Li})$ and, at the same time, lower the Li abundance

peak below the envelope. As a consequence, also the early increase of surface $A(\text{Li})$ during the SGB phase tends to be erased. This mechanism works well for NGC 6397, where $A(\text{Li})$ for TO stars is larger than the value predicted by atomic diffusion models, and the early increase along the SGB is also lower than expected from diffusion (Korn et al. 2006a). The same efficiency of turbulence (i.e. the same reference temperature $\log(T)=6.0$ in the parametrization by R05) however, cannot work for M4 and probably other clusters. Fig. 3 highlights the problem. The solid line represents the value of $A(\text{Li})$ in TO stars, as a function of the metallicity, predicted by our models including atomic diffusion (without radiative levitation) for a reference age of 11-12 Gyr, and starting from the WMAP+BBNS value of $A(\text{Li})$. As discussed in Sect. 8, the lowest metallicity for which these Li predictions are adequate is $[\text{Fe}/\text{H}] \sim -2.0$ dex, since below this value radiative levitation affects appreciably the predicted surface Li abundances (Richard et al. 2002). When TO stars are located above the solid line (as in the case of NGC 6397), atomic diffusion during the MS is too efficient in depleting the Li surface abundance and one can reproduce the observations only by including some form of additional turbulence that brings back to the surface some of the Li diffused out of the convective envelopes, as done by Korn et al. (2006a). For objects located below the solid line – like M4 – however, the inclusion of turbulent mixing with the same efficiency as in NGC 6397 worsens the discrepancy, because it increases the surface $A(\text{Li})$ predicted by fully efficient diffusion.

This suggests that – within the assumption of an initial $A(\text{Li})$ equal to the cosmological value – for the three highest metallicity clusters in Fig. 3, including M4, the turbulence has to reach deeper regions where Li burning occurs (i.e. one needs a higher reference temperature in R05 parametrization of turbulence), and Li-depleted material is dragged to the surface, thus lowering $A(\text{Li})$ below the value expected from atomic diffusion. The same turbulence could also account for the constant Fe abundance observed in our M4 star sample, feeding back to the envelope iron that diffuses below the convection zone during the MS phase.

The observed trend of $A(\text{Li})$ with T_{eff} constrains the shape of the Li stratification in M4 TO stars. The value of $A(\text{Li})$ measured at the TO and its constancy (within the measurement errors) along the early SGB (without the Li peak typical of the Li profile in case of diffusion), plus the constraint given by the efficiency of the Li-burning reactions require a profile like the one displayed as a dot-dashed line in Fig. 9. We have calculated the SGB and RGB evolution starting from a TO model with this 'observationally constrained' Li profile and the abundances of the other elements as in the calculations without diffusion, in the assumption that turbulence has mixed back into the fully mixed envelope the amount diffused below the convection boundary. The resulting surface Li evolution (Fig. 10) reproduces very well the abundance pattern up to the RGB bump, including the $A(\text{Li})$ values along the early RGB.

9.3 Can we really detect the signature of diffusion?

As discussed in Sect. 4, the observed distribution of $A(\text{Li})$ in TO stars is formally compatible with a constant Li value,

⁹ This parametrization makes use of a turbulent diffusion coefficient that is 400 times larger than the diffusion coefficient of He at a reference temperature T , and varies with density (ρ) as ρ^{-3} .

within the measurement errors. In the previous analysis we have therefore considered a constant $A(\text{Li})$ for all TO stars. The question we address here is the following: given the random errors on our estimates of $A(\text{Li})$, is it possible to detect the trend of $A(\text{Li})$ with T_{eff} predicted by models with fully efficient diffusion (dashed line in Fig. 7)? To this purpose, we have created a synthetic sample of $A(\text{Li})$ measurements, drawing randomly 35 values of T_{eff} from the Li-isochrone displayed in Fig. 7, using a flat probability distribution for $T_{\text{eff}} \geq 5900$ K. Gaussian errors equal to our average random observational errors for the TO stars have been then applied to this synthetic sample, and the a F-test as described in Sect. 4 has been performed. This procedure has been repeated 100 times, and for each of these 100 samples the F-test returned a probability below 90% that a spread in $A(\text{Li})$ is present. This means that our measurements of $A(\text{Li})$ cannot rule out the existence of a trend consistent with predictions from models with fully efficient diffusion. If this were to be the case, the observations are matched for an initial $A(\text{Li}) \sim 0.20\text{-}0.25$ dex lower than that the WMAP+BBNS value.

However, a similar test performed on the $[\text{Fe}/\text{H}]$ values predicted by the models with diffusion for whole T_{eff} range of our data, shows that the F-test should be able to detect the expected spread of values, which is contrary to the result for our observed sample. We have verified that the predicted $[\text{Fe}/\text{H}]$ depletion has to be reduced by at least $\sim 70\%$ in order to become undetectable by the F-test, given our random measurement errors. This means that the efficiency of diffusion has to be strongly suppressed by some counteracting turbulence and that the curvature in the Li abundance as a function of T_{eff} for TO stars has to be much lower than what predicted by fully efficient diffusion, if not completely vanishing.

9.4 The initial Li content of M4 stars

The discussion in the previous subsections and the fit displayed in Fig. 10 do not yet allow to identify univocally the pristine $A(\text{Li})$ in M4, because this value is strongly dependent on the details of the adopted turbulent mixing, that seems to play an essential part in the interpretation of the spectroscopic abundances. Two *extreme* situations can be envisaged to obtain the model plotted in Fig. 10:

(i) a pristine $A(\text{Li}) = 2.72$ dex and a turbulent mixing able to reach inner regions where Li is burned, thus dragging to the surface Li-poor material. This solution requires a higher reference temperature in R05 parametrization of turbulence with respect to that proposed by Korn et al. (2006a,b), that does not reach stellar regions where Li is depleted. This solution allows to solve the discrepancy with WMAP+BBNS.

(ii) a pristine $A(\text{Li}) \sim 2.35$ dex and a turbulent mixing qualitatively similar to that of R05 with $\log(T) = 6.09$, showed in their Fig. 7. This efficiency would erase the Li peak at $\log(T) = 6.3$ (see Fig. 9), by increasing the envelope $A(\text{Li})$ back towards the initial value. In this case another possibility to explain the discrepancy with the cosmological Li abundance – apart from inadequacies of the BBNS standard model that could lead to an incorrect estimate of the cosmological $A(\text{Li})$ value (see e.g. Jedamzik & Pospelov 2009) – is to invoke that an amount of primordial Li

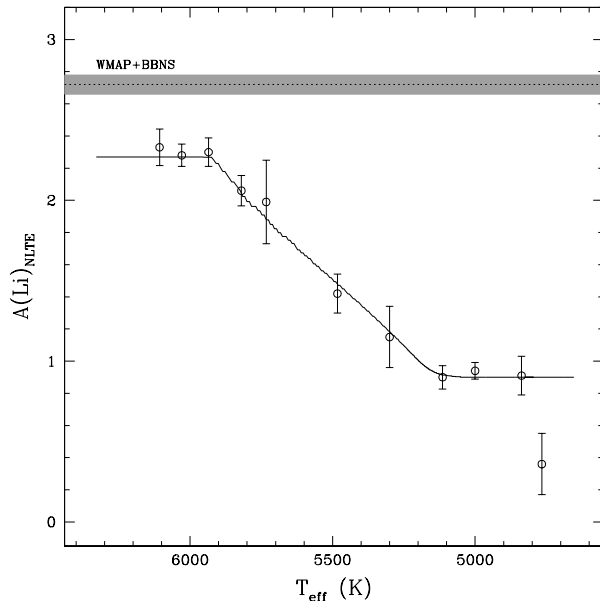


Figure 10. Behaviour of $A(\text{Li})$ as a function of T_{eff} for the stars of M4 (grouped in T_{eff} bins as in Fig. 7), in comparison with the theoretical model computed by adopting the Li profile showed in Fig. 9 as dot-dashed line.

could have been processed by Population III stars, before Population II stars were formed (Piau et al. 2006). The implication in this case is that Population II stars are not ideal to infer the cosmological Li abundance. While this could partially (up to 0.3 dex) solve the discrepancy between the primordial $A(\text{Li})$ and the initial abundance in M4, it also requires a complex and fine tuned scenario. Even if Population III stars have depleted the Li abundance before the cluster formation, some form of turbulent mixing has still to be active below the convective envelope of M4 stars, to erase the $A(\text{Li})$ peak around $\log(T) = 6.3$, that otherwise would produce an increase in the surface $A(\text{Li})$ at the beginning of the SGB evolution.

In light of these considerations, the solution proposed by Korn et al. (2006a), based on R05 parametrization of turbulence with reference temperature $\log(T) = 6.0$ and a initial Li abundance of 2.54 dex, may not be a *universal* solution for the discrepancy with WMAP+BBNS calculations. This value of $\log(T)$ adopted by Korn et al. (2006a) can account for the observations of NGC 6397, but would make the discrepancy worse for M4. Instead, in case of M4 (and possibly also of NGC 6752 and 47 Tuc) one needs a turbulent mixing much deeper than in NGC 6397, that burns a sizable fraction of the initial Li.

10 CONCLUSIONS

We have measured the Li and Fe content for a large sample of stars along different evolutionary phases (TO, SGB and RGB) in the GC M4. The main conclusion of this work can be summarized as follows:

- The Li content in the TO stars of M4 well resembles the Li abundance already observed in other GCs and in the Halo stars, thus confirming the discrepancy with the WMAP+BBNS predictions.

- Qualitatively, the general behaviour of both Li and Fe with T_{eff} is reproduced by models without diffusion, starting from the WMAP+BBNS A(Li) value but we recognize a systematic offset of $\sim+0.3$ dex between the theoretical and the observed Li content along the SGB and RGB stars.

- The behaviour of A(Li) as a function of T_{eff} in TO/SGB stars is incompatible with the theoretical predictions of the models including atomic diffusion, starting from the WMAP+BBNS predicted value; This suggests that an additional turbulent mixing below the convective zone needs to be included in the models.

- The general homogeneity and the value of A(Li) in the TO, early SGB and early RGB stars constrains to the shape of the Li stratification in M4 TO stars. A good match between theoretical models and the global behaviour of the Li abundance as a function of T_{eff} can be obtained by assuming the WMAP+BBNS predicted value plus diffusion and a turbulent mixing reaching regions where Li is burned. The discrepancy with the WMAP+BBNS Li abundance cannot be solved by invoking the same reference temperature for the Richard et al. (2002) parametrization of turbulence, as proposed by Korn et al. (2006a,b) to explain the Li abundance measured in NGC 6397, because in that case the turbulent mixing does not reach layers where Li is burned.

- Different (lower than the WMAP+BBNS predicted value) pristine A(Li) values for M4 are possible, depending on the adopted reference temperature for the turbulent mixing. This uncertainty is mainly due to our poor understanding of the true nature of the turbulent mixing that counteracts the atomic diffusion.

The study of the Li content in M4 points out that the Li problem is far from being solved and new efforts are needed, both to enlarge the number of studied GCs and to refine theoretical stellar and cosmological models. Spectroscopic measurements of A(Li) below the TO would be crucial to put further constraints on the primordial Li in GC stars, given that moving down along the MS - even in case of fully efficient diffusion - one expects to find Li abundances progressively closer to the primordial value. Moreover, a deeper understanding of the nature of the turbulent mixing occurring outside the convective region is needed to disentangle this problem.

We wish to thank Piercarlo Bonifacio and Luca Pasquini for the useful discussions and suggestions. This research was supported by the Agenzia Spaziale Italiana (under contract ASI-INAF I/016/07/0), by the Istituto Nazionale di Astrofisica (INAF, under contract PRIN-INAF2008) and by the Ministero dell'Istruzione, dell'Università e della Ricerca.

REFERENCES

- Ali, A. W., & Griem, H. R. 1965, *Physical Review*, 140, 1044
- Ali, A. W., & Griem, H. R. 1966, *Physical Review*, 144, 366
- Angulo, C., et al. 1999, *Nucl. Phys. A*, 656, 3
- Aoki, W., Barklem, P. S., Beers, T. C., Christlieb, N., Inoue, S., García Pérez, A. E., Norris, J. E., & Carollo, D. 2009, *ApJ*, 698, 1803
- Asplund, M., Lambert, D. L., Nissen, P. E., Primas, F., & Smith, V. V. 2006, *ApJ*, 644, 229
- Barklem, P. S., Piskunov, N., & O'Mara, B. J. 2000, *A&As*, 142, 467
- Bedin, L. R., Salaris, M., Piotto, G., Anderson, J., King, I. R., & Cassisi, S. 2009, *ApJ*, 697, 965
- Boesgaard, A. M., Deliyannis, C. P., Stephens, A., & King, J. R., 1998, *ApJ*, 493, 206
- Bonifacio, P., & Molaro, P. 1997, *MNRAS*, 285, 847
- Bonifacio, P. 2002, *A&A*, 395, 515
- Bonifacio, P., et al. 2002, *A&A*, 390, 91
- Bonifacio, P., et al. 2007, *A&A*, 462, 851
- Bonifacio, P., et al. 2009, *A&A*, 501, 519
- Cameron, A. G. W. & Fowler, W. A. 1971, *ApJ*, 164, 111
- Cardelli, J. A, Clayton, G. C., & Mathis, J. S. 1989, *ApJs*, 345, 245
- Carlsson, M., Rutten, R. J., Bruls, J. H. M. J., & Shchukina, N. G. 1994, *A&A*, 288, 860
- Casagrande, L., Ramírez, I., Meléndez, J., Bessell, M., & Asplund, M. 2010, *A&A*, 512, A54
- Carretta, E. et al., 2009, *A&A*, 505, 117
- Carretta, E., Bragaglia, A., Gratton, R. G., & Lucatello, S., 2009, *A&A*, 505, 139
- Carretta, E., Bragaglia, A., Gratton, R., D'Orazi, V. & Lucatello, S. 2009, *A&A*, 508, 695
- Castelli, F., & Kurucz, R. L., 2003, in *IAU Symposium*, Ed. N. Piskunov, W. W. Weiss & D. F. Gray, 20
- Cassisi, S., Salaris, M., & Irwin, A. W. 2003, *ApJ*, 588, 862
- Castilho, B. V., Gregorio-Hetem, J., Spite, F., Barbuy, B., & Spite, M., 2000, *A&A*, 361, 92
- Cayrel, R. 1988, *The Impact of Very High S/N Spectroscopy on Stellar Physics*, 132, 345
- Chaboyer, B., Demarque, P., & Sarajedini, A. 1996, *ApJ*, 459, 558
- Charbonnel, C., & Primas, F. 2005, *A&A*, 442, 961
- Charbonnel, C., & Lagarde, N., 2010, *arXiv1006.5359*
- Cohen, J. G., & Meléndez, J. 2005, *AJ*, 129, 303
- Cox, J. P., & Giuli, R. T. 1968, *Principle of Stellar Structure* (London: Gordon & Breach)
- Cyburtt, R. H., Fields, B. D., & Olive, K. A. 2008, *Journal of Cosmology and Astro-Particle Physics*, 11, 12
- Decressin, T., Charbonnel, C., Prantzos, N., & Ekstrom, S. 2007, *A&A*, 464, 1029
- D'Orazi, V., Lucatello, S., Gratton, R., Bragaglia, A., Carretta, E., Shen, Z., & Zaggia, S. 2010, *ApJ*, 713, L1
- D'Orazi, V. & Marino, A. F. 2010, *ApJ*, 716 L166
- Drawin, H.-W., 1968, *ZPhy*, 211, 404
- Ferraro, F. R., Messineo, M., Fusi Pecci, F., de Palo, M. A., Straniero, O., Chieffi, A., & Limongi, M. 1999, *AJ*, 118, 1738
- Ferraro, F. R., Sabbi, E., Gratton, R. G., Piotto, G., Lan-

- zoni, B., Carretta, E., Rood, R. T., Sills, A., Fusi Pecci, F., Moehler, S., Beccari, G., Lucatello, S., & Compagni, N., 2006, *ApJ*, 647, 53L
- Fuhr, J. R., Martin, G. A., & Wiese, W. L. 1988, New York: American Institute of Physics (AIP) and American Chemical Society, 1988,
- González Hernández, J. I., & Bonifacio, P. 2009, *A&A*, 497, 497
- González Hernández, J. I., et al. 2009, *A&A*, 505, L13
- Gratton, R. G., Carretta, E., Eriksson, K., & Gustafsson, B. 1999, *A&A*, 350, 955
- Gratton, R. G., Sneden, C., Carretta, E., & Bragaglia, A. 2000, *A&A*, 354, 169
- Gratton, R. G., et al. 2001, *A&A*, 369, 87
- Grevesse, N., & Sauval, A. J., 1998, *SSRv*, 85, 161
- Jedamzik, K., & Pospelov, M. 2009, *New Journal of Physics*, 11, 105028
- Hansen, B. M. S., et al. 2004, *ApJs*, 155, 551
- King, J. R., Stephens, A., Boesgaard, A. M., & Deliyannis, C. 1998, *AJ*, 115, 666
- Korn, A. J., Grundahl, F., Richard, O., Barklem, P. S., Mashonkina, L., Collet, R., Piskunov, N., & Gustafsson, B. 2006, *Nature*, 442, 657
- Korn, A. J., Grundahl, F., Richard, O., Barklem, P. S., Mashonkina, L., Collet, R., Piskunov, N., & Gustafsson, B. 2006, *Msngr*, 125, 6
- Kurucz, R. L., 1993a, *ATLAS9 Stellar Atmosphere Programs and 2 km/s grid*. Kurucz CD-ROM No. 13. Cambridge, Mass.: Smithsonian Astrophysical Observatory, 1993., 13
- Kurucz, R. L., 1993b, *SYNTHE Spectral Synthesis Programs and Line Data*. Kurucz CD-ROM No. 18. Cambridge, Mass.: Smithsonian Astrophysical Observatory, 1993., 18
- Ivans, I. I., Sneden, C., Kraft, R. P., Suntzeff, N. B., Smith, V. V., Langer, G. E., & Fulbright, J. P., 1999, *AJ*, 118, 1273
- Lind, K., Korn, A. J., Barklem, P. S., & Grundahl, F., 2008, *A&A*, 490, 777
- Lind, K., Asplund, M., & Barklem, P. S. 2009, *A&A*, 503, 541
- Lind, K., Primas, F., Charbonnel, C., Grundahl, F., & Asplund, M. 2009, *A&A*, 503, 54
- Lovisi, L., Mucciarelli, A., Ferraro, F. R., Lucatello, S., Lanzoni, B., Dalessandro, E., Beccari, G., Rood, R. T., Sills, A., Fusi Pecci, F., Gratton, R., & Piotto, G., 2010, *arXiv:1007.2343*
- Marino, A. F., Villanova, S., Piotto, G., Milone, A. P., Momany, Y., Bedin, L. R., & Medling, A. M., 2008, *A&A*, 490, 625
- Molaro, P., Bonifacio, P. & Primas, F., 1995, *Memorie della Società Astronomica Italiana*, 66, 323
- Pasquini, L., Bonifacio, P., Molaro, P., Francois, P., Spite, F., Gratton, R. G., Carretta, E., & Wolff, B. 2005, *A&A*, 441, 549
- Piau, L., Beers, T. C., Balsara, D. S., Sivarani, T., Truran, J. W., & Ferguson, J. W. 2006, *ApJ*, 653, 300
- Pietrinferni, A., Cassisi, S., Salaris, M., & Castelli, F. 2006, *ApJ*, 642, 797
- Piotto, G., Zoccali, M., King, I. R., Djorgovski, S. G., Sosin, C., Rich, M. R., & Meylan, G., 1999, *AJ*, 118, 1727
- Richard, O., Michaud, G., & Richer, J. 2002, *ApJ*, 580, 1100
- Richard, O., Michaud, G., & Richer, J. 2005, *ApJ*, 619, 538
- Salaris, M., & Weiss, A. 2001, *A&A*, 376, 955
- Salaris, M., & Weiss, A. 2002, *A&A*, 388, 492
- Sbordone, L., Bonifacio, P., Castelli, F., & Kurucz, R. L., 2004, *Memorie della Società Astronomica Italiana*, 5, 93
- Sbordone, L., et al. 2010, *arXiv:1003.4510*
- Sommariva, V., Piotto, G., Rejkuba, M., Bedin, L. R., Heggie, D. C., Mathieu, R. D., & Villanova, S. 2009, *A&A*, 493, 947
- Spergel, D. N., et al. 2007, *ApJs*, 170, 377
- Spite, M., & Spite, F. 1982, *Nature*, 297, 483
- Steigman, G. 2007, *Annual Review of Nuclear and Particle Science*, 57, 463
- Thoul, A. A., Bahcall, J. N., & Loeb, A. 1994, *ApJ*, 421, 828
- Ventura, P. & D'Antona, F. 2009, *A&A*, 499, 835
- Yan, Z.-C., & Drake, G. W. F. 1995, *Phys. Rev. A.*, 52, 4316
- Weiss, A., & Salaris, M. 1999, *A&A*, 346, 897